The effect of time and surface type on the composition of biofilm communities on concrete exposed to seawater

Citation for the original published paper (version of record):
Karacic, S., Modin, O., Hagelia, P. et al (2022). The effect of time and surface type on the composition of biofilm communities on concrete
exposed to seawater. International Biodeterioration and Biodegradation, 173.
http://dx.doi.org/10.1016/j.ibiod.2022.105458

International Biodeterioration & Biodegradation 173 (2022) 105458

Contents lists available at ScienceDirect

International Biodeterioration & Biodegradation

journal homepage: www.elsevier.com/locate/ibiod

The effect of time and surface type on the composition of biofilm communities on concrete exposed to seawater

Sabina Karačić [a], Oskar Modin [a], Per Hagelia [b], Frank Persson [a], Britt-Marie Wilén [a,*]

[a] Department of Architecture and Civil Engineering, Chalmers University of Technology, Göteborg, Göteborg, Sweden
[b] Tunnel and Concrete Division, The Norwegian Public Roads Administration, Brynsengfaret 6A, 0667, Oslo, Norway

ARTICLE INFO

Keywords:
Microbially induced deterioration
Biofilm
Marine environment
Concrete
Surface structure
Steel fibers

ABSTRACT

Microbially induced deterioration is a threat to concrete infrastructures in marine environments. Complex microbial biofilms form on concrete surfaces exposed to sea water and cause material deterioration. However, the mechanisms determining the composition and the development of the biofilm communities are poorly understood. We designed a mesocosm experiment to determine the influence of concrete surface structure (smooth/rough) and steel fiber reinforcement (presence/absence) on biofilm development over a period of 455 days. This enabled a novel methodology to systematically assess biofilm formation of bacteria on concrete exposed to marine water. The biofilm communities were distinctly different from the planktonic communities in the systems. The alpha diversity increased with time and longer time intervals correlated with higher turnover of taxa. Several taxa within *Caulobacterales* and *Rhodobacterales* were identified as early biofilm formers, which decreased in relative abundance and were replaced by taxa within *Planctomycetales* as the biofilm developed. Throughout the experimental period, concrete surface type influenced the microbial community composition. Some taxa such as *Magnetospiraceae, Portibacter, Rubripirellula*, and *Rhodopirellula*, possibly involved in the oxidation and reduction of iron, were for instance more abundant in biofilms on steel-fiber containing concrete. Null models suggested that mainly deterministic factors were shaping the microbial communities with limited importance of stochasticity at shorter time intervals.

1. Introduction

In marine and fresh waters, microorganisms colonize and form biofilms on biotic and abiotic surfaces (Vishwakarma 2020). This gives the microorganisms survival advantages such as increased nutrient availability, protection from hydration, and increased tolerance to various environmental stressors, which makes biofilms hot spots of microbial activity in nature (Flemming and Wuertz 2019). Biofilm communities have properties that are different from free living bacterial cells with complex microbial interactions (Konopka 2009).

Colonization and subsequent biofilm formation on manmade surfaces can have negative effects such as unwanted biofouling, transmission of harmful microorganisms and biocorrosion (Flemming et al., 2016; Song et al., 2019, Vishwakarma, 2020). For instance, in marine environments, submerged surfaces are rapidly colonized, which can lead to microbially induced deterioration (Wei et al., 2013; Noeiaghaei et al., 2017; Zhou et al., 2021). Bacteria are the main microorganisms involved and early colonizers can determine the structure and function of more mature biofilms (Dang et al., 2011; Dang and Lovell 2016). The nature of the surfaces such as wettability, polarization, tension, and roughness influence biofilm formation (Crawford et al., 2012; Zhang et al., 2014; Caruso 2020; Vivier et al., 2021). Rough surfaces provide protection from unfavorable environments (Mitik-Dineva et al., 2008). Also, the mineral surface composition can be a main factor regulating the biofilm community structure, alpha diversity, and growth (Jones and Bennett 2017). Various concrete mixes have been shown to impact the colonization rate of algae (Natanzi et al., 2021) as well as the composition of bacterial biofilms (Voegel et al., 2020). However, studies investigating the importance of the surface type for biofilm formation are typically conducted in time frames of days or weeks (e.g. Jones et al., 2007; Zhang et al., 2014; Jones and Bennett 2017; Voegel et al., 2020; Hayek et al., 2021; Ryley et al., 2021), and little is known about the long-term succession of the microbial community and the role of surface type for mature biofilms, which is of relevance for manmade structures

* Corresponding author. Department of Architecture and Civil Engineering, Division of Water Environment Technology, Sven Hultins gata 6, SE-412 96, Gothenburg, Sweden.
E-mail address: britt-marie.wilen@chalmers.se (B.-M. Wilén).

https://doi.org/10.1016/j.ibiod.2022.105458
Received 1 October 2021; Received in revised form 28 June 2022; Accepted 28 June 2022
Available online 14 July 2022

persisting in the environment for many years.

On concrete, microbial growth may reduce the pH at the concrete surface due to formation of biogenic acids such as carbonic acid, nitric acid, and sulfuric acid which will transform the cement matrix in the surface region into non-cementitious secondary phases and in extreme cases dissolve it (Bertron 2014). As the degradation proceeds in marine environments, the cement paste is leached and microcracks form. This leads to processes such as ingress of chloride, magnesium and sulfate ions and formation of magnesium silicate hydrate, magnesium hydroxide and sulfate attack, as well as corrosion of steel fibers and steel bars used for reinforcement (Hagelia 2011; Berrocal 2017). The corrosion can be further accelerated by the EPS in the biofilm, containing negative charges that can interact with metals and create galvanic reactions (Beech and Sunner 2004; Torres-Luque et al., 2014).

Knowledge about the detailed mechanisms involved in biofilm formation and the biofilm interaction with the substratum is predominantly based on mechanistic studies using defined cultures of bacteria (see e.g. Dang and Lovell 2016). Such results cannot be directly transferred to natural ecosystems, which have a large diversity of microorganisms with properties and interactions that are hard to predict and where random processes come into play. In community ecology, stochasticity can be defined as random changes in the community structure with respect to species identities and/or functional traits due to stochastic or random processes of birth, death, immigration and emigration, spatiotemporal variation, and/or historical contingency, whereas selection due to fitness differences among microorganisms to environmental conditions and antagonistic or synergistic biotic interactions are considered deterministic factors (Zhou and Ning, 2017). For instance, the microbial attachment to surfaces from a highly diverse pool of planktonic microorganisms is likely, to a large extent, described by stochastic factors (Zhou and Ning 2017). Studies of succession of species abundances over time in ecosystems have also shown that both deterministic factors and stochastic factors are important (Chase and Myers 2011; Dini-Andreote et al., 2015). Only a limited number of studies have investigated biofilm succession in natural ecosystems. For freshwater as well as saline water biofilms, the early stages of succession have been dominated by stochastic factors, while niche-based deterministic factors came into play as the biofilm matured (Veach et al., 2016; Brislawn et al., 2019). Similar patterns were observed for free-floating biofilms in wastewater treatment bioreactors (Liébana et al., 2019). Studies of mature biofilms on fiber reinforced sprayed concrete have furthermore suggested deterministic factors to be important for the community assembly (Karačić et al., 2018). It is, however, unclear whether stochastic or deterministic forces are key determinants for the biofilm succession as it forms and develops on concrete and whether the surface type is an important factor for the succession.

The aim of this study is to assess the main factors that underpin the long-term formation and succession of microbial biofilms on concrete of various surface type exposed to marine water. Our hypothesis is that concrete surface type (rough/smooth concrete surfaces with/without steel fibers) influences the marine microbial biofilm formation. We expect that the composition of marine microbial biofilms forming on concrete are dynamic over time where stochastic factors, like random immigration of microorganisms from the water, have importance for the community assembly at an initial stage and that deterministic factors play a larger role as the biofilm develops.

2. Materials and methods

2.1. Experimental set-up

2.1.1. Mesocosm set-up

The mesocosm was composed of four separate recirculating systems, each consisting of: 1) an upper vessel made of 8 mm thick clear acrylic, 20 × 25 × 53 cm, with a drainage port 10.5 cm from the bottom to maintain a constant volume of water in the vessel (14 L). Each upper vessel was equipped with 18 bottom effluent holes (7 mm) connected to tube regulators for flow control at 2 mL/min; 2) a middle vessel, 15 × 22 × 53 cm (17.5 L) with a bottom drainage pipe; and 3) a bottom container of 25 L (Fig. S1). The water was recirculated from the bottom container to the upper vessel at 9 L/h by a peristaltic pump. The water was evenly distributed over the inclined surface of each concrete block.

Seawater from 70 m depth was collected at Kristineberg Marine Research Station (University of Gothenburg) in Fiskebäckskil, Sweden. During collection, the sea water was filtered through a 50 μm filter for removal of debris and larger organisms. Every 2–6 weeks (average 3 weeks) the water in the mesocosm (denoted "water from systems 1–4") was replaced with new sea water (denoted "seawater") to provide the system with inoculum. To compensate for evaporation, sterile ultrapure water (Milli-Q) was added to maintain constant volume in the systems. The mesocosm set-up was kept at 13 °C and placed in a dark room to avoid growth of algae. At regular intervals, pH and conductivity was measured in the system (WTW Multiliner 363IDS). The water was saturated with oxygen through recirculation of water in contact with the atmosphere. This set-up allowed for investigation of how biofilms formed on the concrete surfaces subjected to water flow, but also on how the concrete affected the water chemistry in the four systems.

2.1.2. Concrete composition and description of the different treatments

The concrete mix was made with 5% microsilica ELKEM grade 920 added to RAPID Aalborg cement. Sand of $D_{max} = 0.4$ mm was used for a high water/binder ratio of 0.80 with high permeability (prepared with tap water) in order to speed up concrete degradation. With the exception of the high water/binder-ratio, the concrete mix was similar to the ones used in the construction of a subsea road tunnel (Karačić et al., 2018). One batch of 20 L concrete mix was prepared with addition of steel fibers, (0.8 kg·m^{-3}) GSF 0520 which also contains small amounts of Zn, P, K, Ca, Mg, Si, O and C, and another batch without steel fibers. The concretes were cast in 10 × 10 × 10 cm standard wooden molds (EN 12390-1). After demoulding, the concrete blocks were cut diagonally into triangular prisms using a diamond blade. Thereafter, half of samples were sand blasted to increase the surface roughness. All concrete pieces were stored in sterile ultrapure water (Milli-Q) for 30 days prior to starting the experiment to cure the concrete matrix and to wash away debris from sand blasting. A total of 72 triangular prisms were divided in four systems: 1) smooth concrete surface without steel fiber reinforcement 2) smooth concrete surface with steel fiber reinforcement 3) rough concrete surface without steel fiber reinforcement 4) rough concrete

Table 1
Characteristics of the concrete (presence/absence of steel fiber reinforcement and surface structure) and chemical composition of the water in systems 1–4 and in the seawater. Concentrations of other ions and statistical analysis are shown in the supplementary material (Table S1).

Parameter	System 1	System 2	System 3	System 4	Seawater
Reinforcement	no fiber	steel fiber	no fiber	steel fiber	-
Surface structure	smooth	smooth	rough	rough	-
pH (of water)	8.32 ± 0.08	8.36 ± 0.07	8.35 ± 0.07	8.38 ± 0.075	8.18 ± 0.12
Conductivity (mS cm^{-1})	52.93 ± 1.70	52.81 ± 1.36	53.22 ± 1.30	53.89 ± 1.65	50.41 ± 1.07
Alkalinity (mgHCO_3 l^{-1})	126 ± 14	130 ± 4	123 ± 7	135 ± 9	102 ± 15
DOC (mg l^{-1})	4.32 ± 2.21	5.23 ± 3.27	4.84 ± 2.80	4.27 ± 2.87	2.65 ± 1.38
N_{tot}(mg l^{-1})	0.068 ± 0.067	0.100 ± 0.079	0.092 ± 0.073	0.066 ± 0.053	0.066 ± 0.066
Ca (mg l^{-1})	503 ± 100	513 ± 152	471 ± 113	464 ± 128	458 ± 175
Si (mg l^{-1})	2.361 ± 1.310	2.187 ± 1.074	2.212 ± 1.257	2.137 ± 1.207	1.909 ± 1.027
Fe (mg l^{-1})	0.214 ± 0.023	0.216 ± 0.015	0.202 ± 0.023	0.216 ± 0.026	0.217 ± 0.024

surface with steel fiber reinforcement (Fig. S2, Table 1).

2.1.3. Sampling

The mesocosm was operated for 455 days (65 weeks). At each sampling occasion, triplicate concrete pieces were taken out (handled with sterile gloves to avoid contamination) and stored at −20 °C until DNA extraction. Sampling was conducted after 147, 245, 301, 357 and 413 days. The last triplicate samples from day 455 were used for SEM-analysis and no DNA was extracted. Photos were taken of every concrete piece of pristine concrete and at each sampling occasion to follow microbial colonization and change in concrete appearance. For DNA extraction, the concrete surface of each sample was scraped off with a sterile scalpel and collected in DNA-free tubes (performed in a sterile UV-disinfected cabin). For SEM analysis, concrete samples with biofilm were cut in small pieces (≈1 cm^2) with diamond saw with water as coolant, and in some cases biofilm with concrete material was carefully peeled off using a scalpel.

Filtered (0.2 μm) water samples were collected at every water replacement of the mesocosm from systems 1–4 and from the new seawater. The water samples were stored at −20 °C for subsequent analysis. Planktonic microorganisms in the seawater and water from the mesocosms (0.4–1 L) were collected on 0.2 μm membrane filters (Sartorius Stedim Biotech, 47 mm), which were stored at −20 °C for DNA extraction.

2.2. Analytical methods

2.2.1. Chemical analyses

In the filtered water samples, selected metals were quantified by quadrupole Inductively Coupled Plasma. Mass Spectroscopy (ICP-MS) using an iCAP Qc (Thermo Fisher Scientific, Wilmington, DE, USA) and dissolved ions were analyzed using a Dionex ICS-900 ion chromatograph. Dissolved organic carbon (DOC) and total nitrogen in filtered water samples were measured using a Shimadzu TOC-V analyzer. Alkalinity was measured (TitroLine®7000) according to standard methods (APHA 1998).

2.2.2. Scanning electron microscopy (SEM)

Small pieces of selected concrete samples were mounted on a metal stub for SEM. Pristine and uncoated samples were investigated under high-vacuum mode at an acceleration voltage of 20 kV, spot size of 5 μm, and a working distance of 10.2–14.3 mm using a Quanta200 ESEM (FEI). The Oxford Inca Energy Dispersive X-ray (EDX) was used for chemical characterization and chemical point analysis. Data analysis was performed using the INCA EDS software. Other samples were analyzed in a Hitachi S–3600N Scanning Electron Microscope (SEM) available at the GeoLAb, Natural History Museum, University of Oslo. The instrument is equipped with a Bruker XFlash® 5030 energy dispersive X-ray detector (EDX), running on Quantax 400 (Esprit 1.9), for semi-quantitative elemental analysis and hyperspectral mapping, with <127 eV FWHM at MnKα energy resolution. Samples were mounted on carbon tape and analyzed in variable pressure (VP) mode (20 Pa), 15.0 kV accelerating voltage, ca 50 nA beam current.

2.2.3. DNA extraction, amplification, and sequencing

A total of 60 concrete samples and 47 membrane filters (0.2 μm) were collected for DNA analysis. Total genomic DNA was extracted using the Fast DNA spin kit for soil (MP Biomedicals) following the manufacturer's protocol. The V4 hyper-variable region of the 16S rRNA gene was amplified in duplicates, using the forward primer 515′F and the reverse primer 806R (Caporaso et al., 2011; Hugerth et al., 2014) to cover both bacteria and archaea. The primers were indexed according to Kozich et al. (2013). PCR was conducted in 20 μl reactions using the Phusion Hot Start II DNA Polymerase (0.2 μl) (Thermo Scientific), 5X Phusion HF Buffer (4 μl), 10 mM dNTPs (0.4 μl), DMSO (0.6 μl), genomic DNA (1 μl), and 1 μl of each of the forward and reverse primers (10 μM). The PCR was carried out as follows: initial denaturation at 98 °C for 30 s, denaturation at 98 °C for 10 s, annealing at 55.8 °C for 30 s, and extension at 72 °C for 30 s for 30 cycles, followed by final extension at 72 °C for 10 min. The duplicate PCR products were quality checked by standard gel electrophoresis, pooled and purified with the MagJET NGS Cleanup and Size Selection Kit (Thermo Scientific). The DNA concentration was measured using a Qubit 3.0 fluorometer (Invitrogen) with the dsDNA HS assay kit (Invitrogen). The PCR products were pooled in equimolar amounts and the quality was confirmed using TapeStation (Agilent Technologies). Sequencing was performed on an Illumina MiSeq using reagent kit v3. Raw sequence reads have been deposited in the NCBI Sequence Read Archive: BioProject PRJNA747171, accession number SUB10009856.

2.2.4. Bioinformatics and statistical analysis

The sequence reads were processed using the VSEARCH v.2.13.1 (Rognes et al., 2016) and DADA2 v.1.16 (Callahan et al., 2016) pipelines, which determine amplicon sequence variants (ASVs). Based on the VSEARCH and DADA2 count tables, a consensus table of ASVs detected in both pipelines was generated using qdiv (Modin et al., 2020). Taxonomy was assigned with SINTAX (Edgar 2016) within VSEARCH using the Silva database v.132 (Quast et al., 2013). The dataset was rarefied by subsampling each sample to 17879 reads.

Alpha and beta diversity was calculated using the Hill number framework, which allows a systematic evaluation of the impact of relative abundance on diversity measures (Chao et al., 2014; Jost 2006). The parameter q is the diversity order. At a q of 0, all ASVs are considered equally important irrespective of their relative abundance. At a q of 1, each ASV is weighted according to its relative abundance in a sample. For alpha diversity (^{q}D), this means that ^{0}D is equal to the number of ASVs found in a sample (richness) while ^{1}D can be interpreted as the number of "common" ASVs. The corresponding dissimilarity index (^{q}d) shows the fraction of all (^{0}d) and common (^{1}d) ASVs not shared between a pair of samples (Jost 2007; Modin et al., 2020).

Null models were used to determine the dissimilarity caused by compositional turnover between samples and to assess the roles of deterministic and stochastic factors for microbial community assembly. For this, the Raup-Crick null model (Chase et al., 2011; Raup and Crick 1979) adapted for Hill-based dissimilarities (Modin et al., 2020) was used. Permanova (9999 permutations) was used to assess the statistical significance of differences between groups of samples (Anderson 2001). PICRUSt2 was used to predict metabolic functions of the microbial communities based on the 16S rRNA gene sequences (Douglas et al., 2020). The pipeline was run with default settings and the relative abundances of MetaCyc pathways were determined for each sample (Caspi et al., 2020).

Data visualization, ordination, calculation of alpha and beta diversity, null modelling, and permanova tests were conducted in qdiv. Univariate statistical tests (Two-way Anova, Levene's and Shapiro-Wilk's test and post-hoc Games-Howels test) were performed using the Real Statistics add-in to Excel. The DESeq2 method (Love et al., 2014) to test differential abundance of ASVs with time and between systems was carried out in R (R Core Team, 2020). Details about the analysis are provided in the supplementary methods.

3. Results

3.1. Biofilm growth on the concrete

This study consisted of four treatments with concrete surfaces with/without steel fibers and with/without treatment to increase surface roughness (Table 1, Fig. S2). A thin, slightly slimy layer of biofilm was formed on all concrete surfaces (Fig. 1). In the presence of steel fibers, orange deposits also appeared. However, there was no visible difference in biofilm appearance on the smooth and rough concrete surfaces.

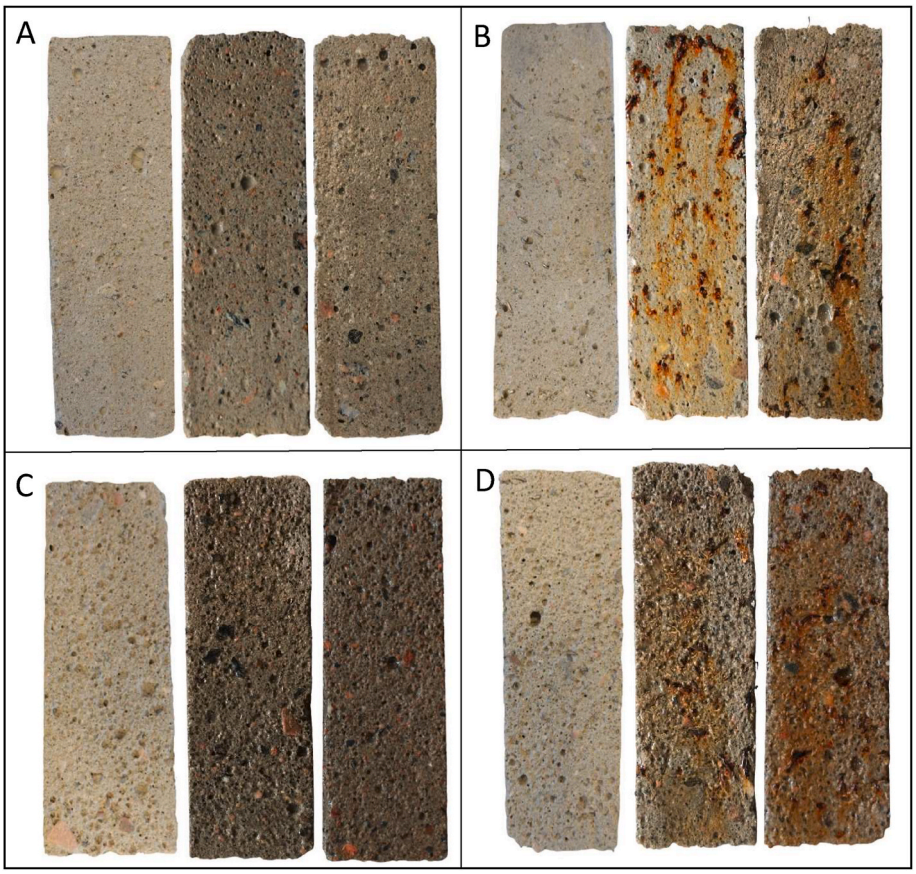

Fig. 1. Concrete blocks from system 1 (A), system 2 (B), system 3 (C), and system 4 (D). The three blocks from each system are sampled on day 1 (left), day 301 (middle), and day 413 (right).

3.2. Signs of degradation of the concrete surfaces

Selected concrete samples were examined by SEM to indicate microbial cells and mineral transformations on the concrete surfaces. Microorganisms were observed on both concrete with and without steel fibers, while secondary deposits were omnipresent on the surfaces with steel fibers (system 4) but were less visible on the surfaces without (system 3) (Fig. S3). At day 357, system 3 was characterized by significantly calcium-leached cement paste as indicated by very low Ca/Si ratios and tiny aggregate particles being separated from the paste in an otherwise porous matrix (Fig. S6). At day 455, system 4 showed several additional features with heavily mineralized constituents consisting of iron hydroxide or iron oxyhydroxide with variable contents of Al, Si and Mg (Fig. S4) as well as domains without Fe (Fig. S5). In some domains the composition resembles magnesium-silicate hydrate with additional Si and Al (Magnesium-aluminum-silicate hydrate, MASH) suggesting impact of cement paste transformations. There was a notable scarcity/absence of Ca in the deposits, suggesting that Ca might have been dissolved into the water phase (Figs. S4 and S5).

3.3. Chemical composition of the water

The chemical composition of the seawater and the water that had percolated over the concrete blocks in systems 1–4 is summarized in Table 1 and Table S1. For the ions, metals, and dissolved organic carbon (DOC), the concentrations were not significantly different between the water systems, indicating that the experiment had minor effect on these parameters. However, the water in systems 1–4 had significantly higher pH, alkalinity, conductivity, and DOC compared to the sea water (Table 1) although the average values were in the same range. Especially for pH, differences between the systems also indicated that the iron fibers and surface structure had an impact (significant difference between system 1 and 2, system 3 and 4 as well as between systems 1 and 3, $p < 0.05$, Table S2). There was a linear correlation between DOC and total nitrogen which may indicate microbial growth ($r^2 = 0.80$, $p = 0.04$). In addition, the differences over time in the concentration of several of the ions, metals, and DOC, as well as of pH and conductivity were significant ($p < 0.05$), likely reflecting the seasonal changes of the seawater (Table S2, Fig. S7). The higher pH at the start of the experiment could be due to dissolution of cementitious material, followed by a levelling off and a subsequent increase during the last part of the experiment.

The dissolution of the cement matrix was assessed by calculating the cumulative concentrations of the chemical constituent in the water of the systems with time. For some of the constituents, an increase in cumulative concentrations was observed. Systems 2 and 4 had higher cumulative increase in alkalinity, whereas the systems 1 and 3 had higher cumulative increase in conductivity (Fig. S8). The increase in cumulative alkalinity shows that carbonate containing constituents have dissolved from the cement matrix. The increase in cumulative conductivity reflects the release of various ions to the water phase. For some ions, Ca^{2+}, SO_4^{2-}, K^+ and the metal Cr, which are constituents of concrete, the cumulative concentrations increased with time (Fig. S8), whereas no or even negative cumulative concentrations were observed for the ions Cl^-, Na^+, Mg^{2+}, and metals V, Mn, Fe, Co, Ni, Cu, Zn, and Cd.

3.4. Alpha diversity of the microbial communities

Alpha diversity was measured at the diversity order of 0 (^0D), equivalent to richness giving equal weight to all ASVs, and 1 (^1D), taking the relative abundances of the ASVs into account. Across all four systems, alpha diversity of the biofilm communities increased over time for

both ^{0}D and ^{1}D (ANOVA, $p < 0.001$ and $p < 0.01$, respectively) (Fig. 2). Although alpha diversity was also different between the four types of biofilm (B1–B4) for both ^{0}D and ^{1}D (ANOVA, $p < 0.01$), post-hoc testing could not separate the biofilm types (Games-Howell, $p > 0.05$), indicating that this pattern was of minor importance. The alpha diversity of the biofilm communities was higher (Fig. 2) than the diversity of the planktonic communities (Fig. S9).

3.5. Beta diversity of the microbial communities

Small fractions of ASVs were entirely unique to the biofilm communities on the concrete of different types or to the planktonic communities, based on Venn diagrams (Fig. S10), with a total of 1206 ASVs (92% of reads) being shared between all sample types over all time points. Although most ASVs appeared in all sample types, their relative abundances differed. As a consequence, the biofilms and the planktonic microorganisms in the seawater and the water in the systems 1–4 formed three distinct microbial communities (Fig. 3A) with significant differences between the three groups ($p = 0.0001$, Permanova). The changes in biofilm community composition during the experiment are shown in Fig. 3B. There was a significant difference in composition between the four concrete types ($p = 0.0001$, Permanova), but all biofilm communities followed a similar temporal trajectory. Incidence-based dissimilarity indices (^{0}d, Fig. S11) showed the same pattern as the relative abundance-based dissimilarity (^{1}d, Fig. 3). The planktonic microbial communities also followed a temporal trajectory but the separation between the four systems was not as clear as for the biofilms, although a significant difference could be observed with the ^{0}d index (Fig. S12).

The biofilm communities clustered based on the presence/absence of steel fibers in the concrete as well as the surface structure of the concrete (smooth/rough). The dissimilarity between samples collected from concrete surface with and without steel fibers were consistently significantly higher than the dissimilarity between samples from rough and smooth surface, which in turn had higher dissimilarity than the replicate samples (Fig. 3C).

Time was an important parameter affecting biofilm community composition. Longer time difference between two samples correlated with higher dissimilarity (Fig. 3D). The temporal rate of change in community composition in the biofilms was determined by dividing the dissimilarity between a pair of samples from a system with the time difference (in days) between the samples. The Bray-Curtis dissimilarity index was used to allow comparison to a previous meta-study, which used this index to describe temporal changes in microbial community composition in various environments (Shade et al., 2013). The Bray-Curtis index gives high weight to the relative abundance of ASVs and is therefore quite insensitive to changes occurring among low-abundant ASVs. The rate of change ranged from 0.0081 ± 0.0015 d^{-1} (avg. $\pm$ st. dev.) for a time difference of 56 d, to 0.0031 ± 0.0001 d^{-1} for a time difference of 266 d (Fig. S13).

Microbial community assembly of the biofilms was assessed using the Raup-Crick null model (Raup and Crick 1979). This null model fixes the richness in each sample, which means that dissimilarities between samples observed are caused by compositional turnover, not by richness differences. It also gives an indication whether deterministic or stochastic processes drive community assembly (Chase et al., 2011). In the null model, the microbial community composition of each sample is reconstructed by randomly drawing ASVs from a regional pool and populate them with read counts (Stegen et al., 2013). This is repeated multiple times and each time, pairwise dissimilarities are calculated between the randomly generated sample communities. These null model dissimilarities are then compared to the observed dissimilarities between the real samples. The null model results (^{q}RC) are reported as an index constrained between 0 and 1. A value close to 0 means that two samples have higher compositional similarity than the null expectation, and a value close to 1 means that the compositional turnover is greater than the null expectation. Intermediate values indicate the dissimilarity between samples can be explained by random assembly (Modin et al., 2020). The definition of the regional pool from which ASVs and read counts are drawn is crucial for the interpretation of the null model results.

We considered all biofilm samples to be part of the regional pool. Fig. 4 shows how time differences between samples from the same system affected the null model results. For the incidence-based index (^{0}RC), the value is 0 for time differences less than approximately 150 days. This means that when it comes to presence/absence of ASVs, the compositional similarity is much higher than what would be under a random assembly process. The relative abundance-based index (^{1}RC) has intermediate values, which means that the difference in relative abundance between the detected ASVs could be explained by random processes. At longer time intervals (>250 d), the ^{0}RC index has intermediate values or is close to 1 in some systems. The ^{1}RC is close to 1 in all systems. This means that there has been a significant change in the identity of ASVs and especially in the relative abundance of ASVs. A comparison of null model results between systems showed that at all time points, the ^{0}RC was close to 0 and the ^{1}RC had intermediate values (Fig. S14). This suggests that it is primarily time that drives turnover in community composition in the biofilms. Turnover caused by different concrete surface in the four systems is small in comparison, and the biofilms in all four systems follow the same temporal trajectory. This agrees with the PCoA ordination of the biofilm communities on the four concrete types over time (Fig. 3B).

3.6. Microbial community composition

The most abundant taxa, grouped by order, are shown in Fig. 5. The development of the biofilm communities appears to be synchronized in

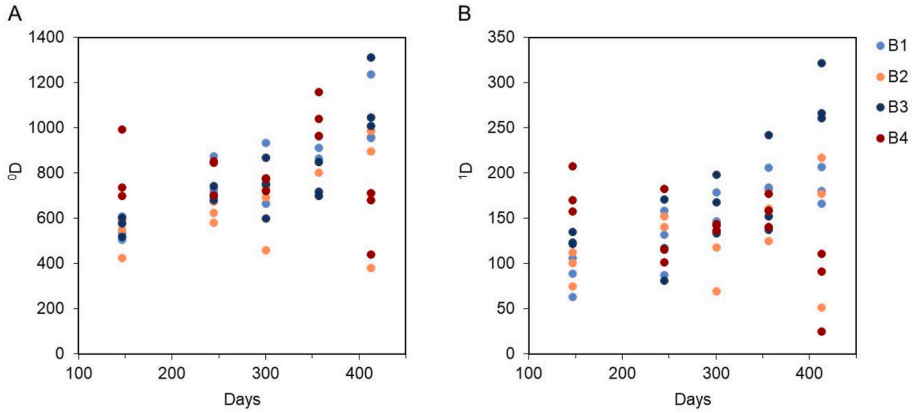

Fig. 2. Alpha diversity of biofilm samples over time for the different treatments (B1–B4). Diversity (D) as Hill number with diversity order 0 (A) and 1 (B).

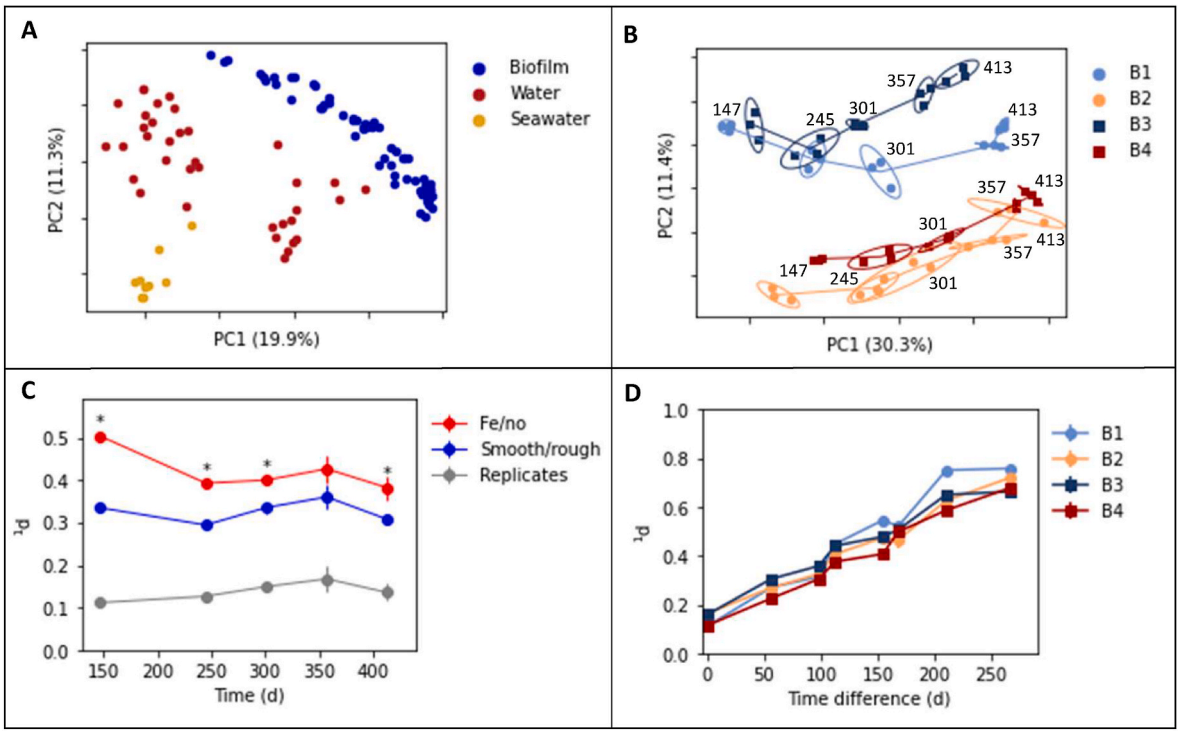

Fig. 3. Beta diversity based on ^{1}d dissimilarities. (A) PCoA of all samples in the study. (B) PCoA of the biofilm samples, where the ellipses encircle replicate samples from the same time point. The time point (day of the experiment) is denoted at each ellipse. (C) Dissimilarities between the biofilm samples of replicates (grey), concrete surfaces with different roughness (blue), and concrete with and without iron fibers (red). The average and standard error of pairwise dissimilarities are shown. Asterisks (*) indicate that the dissimilarity between samples from concrete with and without iron fibers is significantly greater than the dissimilarity of samples from concrete with different roughness ($p < 0.05$, Welch's *t*-test). (D) The effect of time difference on dissimilarities. Each point shows the average of several pairwise dissimilarities. Error bars show standard error (too small to be seen in the graph). At a time-difference of 0, the ^{1}d represents dissimilarity between biological replicates.

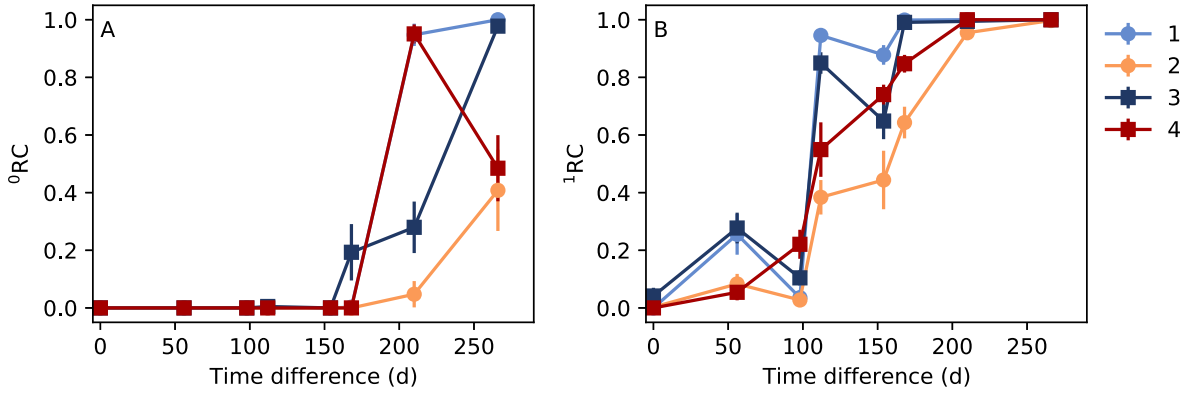

Fig. 4. Null model results (^{q}RC) for the incidence-based based dissimilarity index (A, ^{0}d) and the relative-abundance based dissimilarity index (B, ^{1}d). The x-axis shows the time difference between the samples being compared. The average value of pairwise comparisons of samples from the same system are shown. The error bars show the standard error of the mean.

the four systems, which is in agreement with Fig. 3B. *Caulobacterales* and *Rhodobacterales* decrease in relative abundance over time while *Planktomycetales*, *Rhizobiales*, and *Pirellulaes* show increasing trends. Similar temporal trends for the mentioned orders are seen in the water samples. However, some orders such as *Cellvibrionales*, *Salinisphearales*, and *SAR86 clade* appear in higher relative abundance in the water samples in comparison to the biofilms. Some orders, most notably *Marine Group II* and *Nitrosopumilales,* have high relative abundance in the seawater but they do not remain in the laboratory mesocosm.

To investigate how time, steel fiber content, and surface structure affected the abundance of individual ASVs in the biofilms, DESeq2 was used (Love et al., 2014). Fig. 6 shows ASVs with statistically significant differences in abundance between sample types and over time ($p < 0.001$). The ASVs are grouped based on genus and only ASVs with a log2 (fold-change) of at least 2 and a relative abundance exceeding 0.5% in at least one sample are shown. For the time variable, the log2(fold-change) refers to the change in abundance occurring over one year of biofilm development. In total, 72 ASVs changed significantly in abundance with time. These could be grouped according to taxa. Within *Planctomycetales* and *Rhizobiales*, all ASVs increased over time. Even within *Rhodobacterales*, there were also many ASVs that increased over time. The overall decrease seen in Fig. 5 is driven by *Roseobacter*, which is an abundant genus within that order. A similar phenomenon is seen for the ASVs belonging to *Pirellulales*. Within *Caulobacterales*, most ASVs

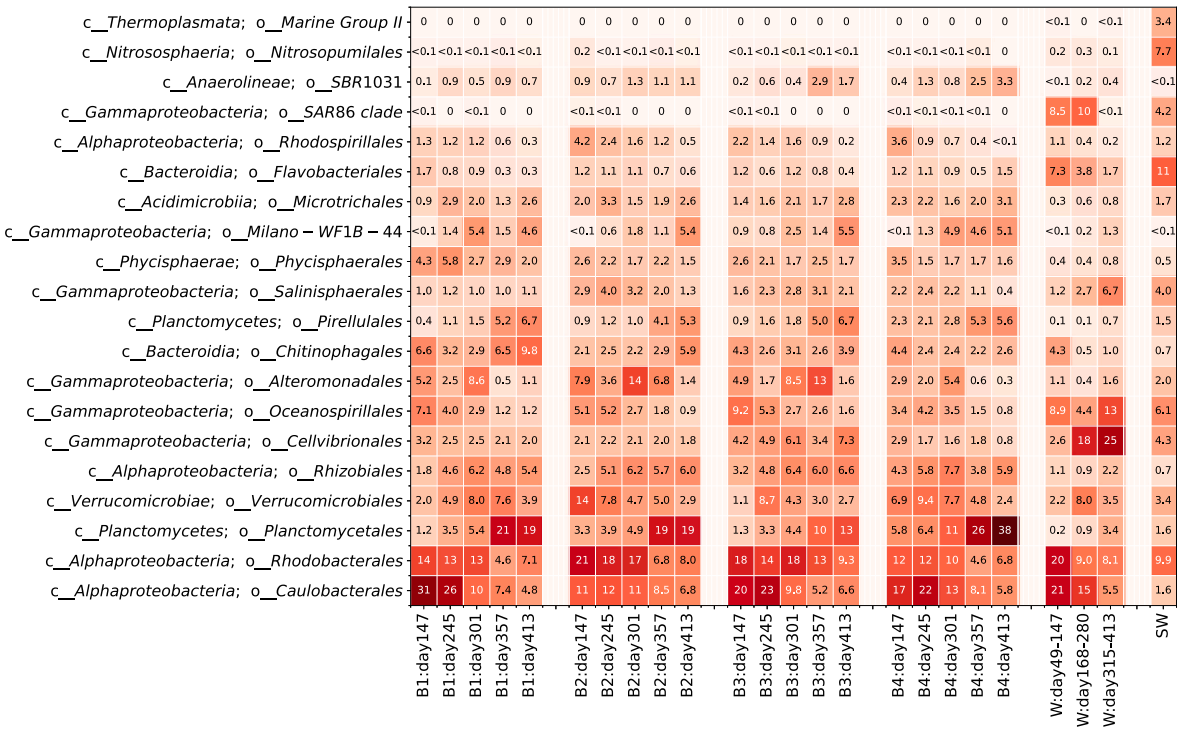

Fig. 5. The 20 most abundant orders in the microbial communities. The colour bar indicates percentage relative abundance in the samples. For the biofilms (B1–B4) triplicate samples were merged. For the water samples, samples were merged into three groups representing the early phase (day 49–147), the middle phase (day 168–280) and the later phase (day 315–413). For the sea water (SW), all samples were merged.

decreased in abundance with time, which is consistent with Fig. 5. However, one genus, *Hyphomonas*, have ASVs that both increase and decrease with time. The same phenomenon can be observed for ASVs classified as *OM190*, *Rhodobacteraceae*, and *Glaciecola*. Furthermore, 10 and 38 ASVs were different in abundance based on the surface structure of the concrete and the presence/absence of steel fiber reinforcement, respectively (Fig. 6). Examples of taxa that appeared to favor steel fiber-containing concrete were *Magnetospiraceae*, *Portibacter*, *Rubripirellula*, and *Rhodopirellula*.

Of the ASVs that decreased with time, most were more abundant in biofilm than in water indicating they were early biofilm forming bacteria (Fig. 6). Overall, 81 ASVs were significantly more abundant in the biofilms and only 7 ASVs were more abundant in the water ($p < 0.05$, DESeq2, Table S3), which also reflects the higher alpha diversity of the biofilm samples (Fig. S9). All ASVs showing significant differential abundance based on DESeq2 analysis are shown in Tables S3–S6.

4. Discussion

Microorganisms can provide us with both ecosystem services and disservices (Lyytimäki et al., 2008). Microorganisms intentionally embedded in concrete can contribute to increased durability due to self-healing effects (Nathaniel et al., 2020), while microbial biofilms forming on the concrete surface typically contribute to reduced performance and lifespan by disintegration of the surface material (Noeiaghaei et al., 2017). A fundamental understanding of how such biofilms form and how the community members succeed on the surfaces is key for assessment of the degradation.

4.1. Early biofilm development

Even though biofilm on the concrete was composed of typical marine taxa, the biofilm community composition was distinctly different from the planktonic composition in the flowing water and the seawater (Fig. 3A). The compositional differences between replicate biofilm samples were much smaller than could be explained by stochasticity (see time zero in Fig. 4), which suggests that deterministic forces, like environmental conditions, were important for shaping the biofilm community. This can be exemplified with the concrete surface types, where the dissimilarity was considerably larger between biofilm communities on different surface types than between replicates within each surface types (Fig. 3C). This also confirms observations in other ecosystems (Ali et al., 2019; Besemer et al., 2012), that biofilm formation primarily depends on species traits and environmental conditions, rather than random mass immigration from the water phase.

Several of the taxa that had significantly higher abundance in the biofilms than in the water showed a decreasing trend in the biofilms (see black squares in blue circles in Fig. 6). This indicates that they were early biofilm forming bacteria on the concrete and conditioned the surface for subsequent microorganisms. Over time, the early biofilm formers decreased in relative abundance because of competition from invading species. Hence, being an early biofilm former did not spur long-term abundance, which is in line with findings in other biofilms (Brislawn et al., 2019). In this study, species within a number of taxonomic orders served as such early biofilm formers (Fig. 6 and Fig. S15). *Ponticaulis* sp. and *Hyphomonas* sp. were two of the most abundant genera and have previously been found to play important roles in biofilm formation on steel in marine environments (Procópio 2020). A *Roseobacter* clade has previously been detected in high abundances in biofilms forming on SiO_2 surfaces after short-term (2.5 weeks) exposure in the sea (Sanli et al., 2015). Similarly, *Blastopirellula* sp. have been shown to preferentially colonize and form biofilms on SiO_2 immersed in the sea for one week (Wang et al., 2020), supporting that these two bacterial taxa are important in early-stage biofilm formation in marine environments.

4.2. Succession of the biofilm community

Time was the major factor shaping the biofilm communities (Fig. 3B, D). In the succession, many of the ASVs that were abundant in the early phase decreased in relative abundance (Fig. S15) as other ASVs

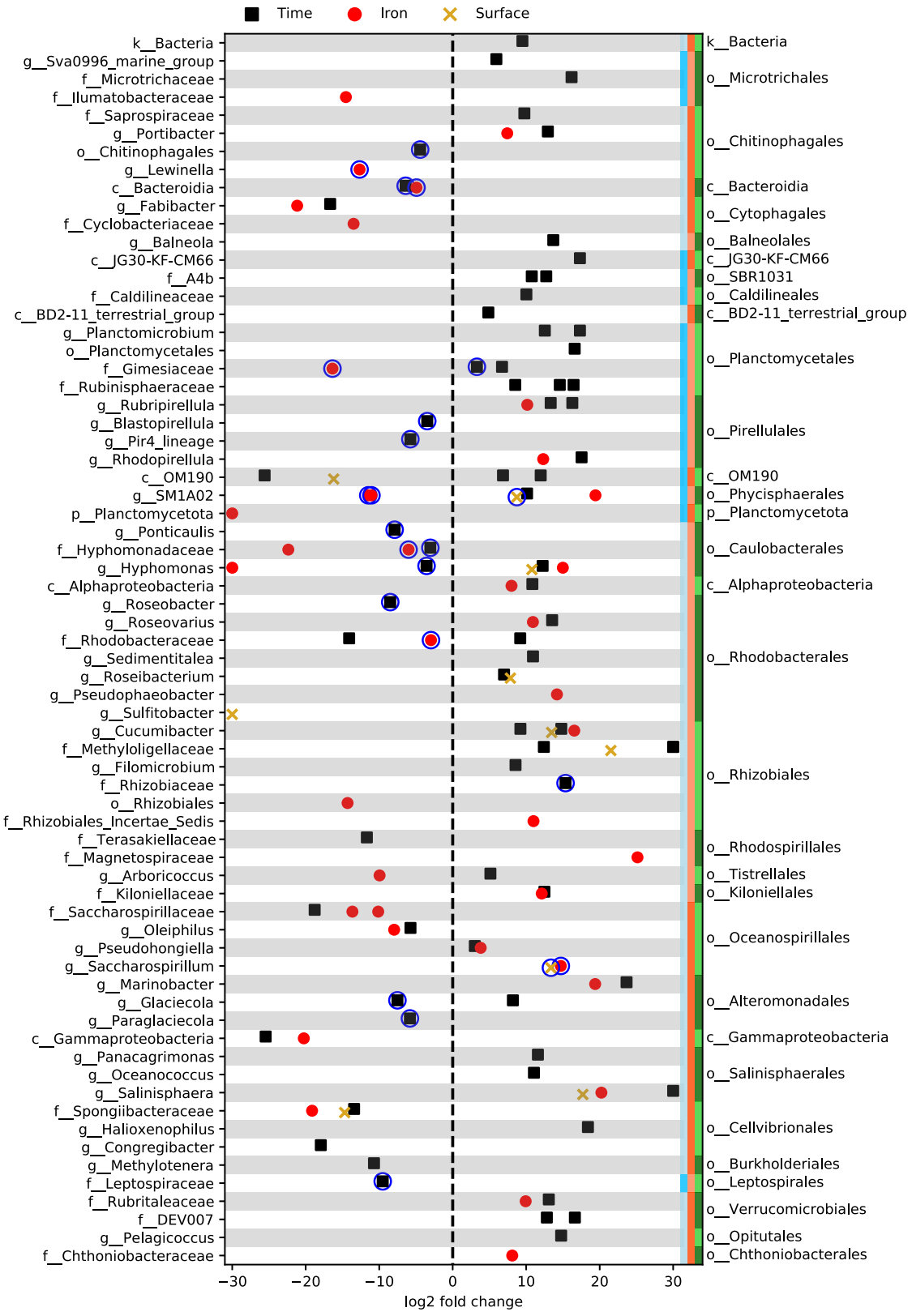

Fig. 6. ASVs with significant differential abundance based on DESeq2 results ($p_{adj} < 0.001$). Positive log2(fold-change) means that the ASV increased in abundance with time (black squares), had higher abundance on steel fiber containing surfaces (red circles), or had higher abundance on smooth surfaces (orange X). Each point represents one ASVs. They are grouped based on genus classification on the left y-axis. The right y-axis shows taxonomic order. The red/pink and blue/light blue bars on the right x-axis shows how the orders are grouped into classes and phyla, respectively. If a point is surrounded by a blue circle, it means that ASV had a significantly higher abundance in the biofilm in comparison to the water samples ($p_{adj} < 0.05$).

increased (Fig. S18) and the biofilm communities developed and gradually became more diverse (Fig. 2). Previous studies report different diversity patterns during biofilm community development. Jackson et al. (2001) observed elevated richness during initial colonization, which was followed by a slight decrease in richness as a result of competition and limited niche availability. Then, as the biofilm matured, more niches became available which permitted growth of a larger variation of species resulting in increased alpha diversity. Other studies of biofilms have shown linear increases of richness and alpha diversity over time (Redford and Fierer 2009; Veach et al., 2016) which follow general patterns of species-time relationships observed in many microbial ecosystems (Shade et al., 2013). Deterministic forces of species interactions and environmental filtering are likely an important explanation for the increase in diversity over time. As the biofilm develops, microorganisms able to utilize extracellular polymers and metabolic by-products find niches within the biofilm (Datta et al., 2016). The long-term exposure of the concrete to sea water also causes changes in physical-chemical properties, which can change the environmental niches and cause changes in the microbial community (Caruso 2020). The biofilms observed were very thin, appeared as a slimy layer probably consisting of a hydrated matrix of extracellular polymeric substances (Fig. 1) (Flemming et al., 2016). Thin biofilms give rise to low diffusion resistance and hence absence of distinct chemical niches, such as anaerobic zones, where more metabolically diverse microorganisms can proliferate (Stewart 2003). With time, a thicker biofilm would probably have formed, resulting in an even more diverse microbial community.

The temporal rate of change in biofilm community composition (Fig. S13) was the same as those determined for microbial communities in lakes, freshwater streams, air, wastewater treatment plants, marine environments, soil, flowers, and humans for similar time intervals (Shade et al., 2013), suggesting that at time scales of several months microbial community changes are generally gradual with little drastic events. Even so, there was indeed turnover of taxa within the biofilm communities over the longer time intervals, as shown by the null models (Fig. 4). This also indicates that deterministic forces (species interactions and environmental filtering) were important for shaping the microbial community composition over the longer time intervals, while at shorter ones, stochastic immigration/emigration and drift were having a somewhat larger influence, which supports recent findings of succession in other biofilm systems (Liébana et al., 2019; Veach et al., 2016; Brislawn et al., 2019).

For some taxa, we could see that one ASV was replaced by another ASV within the same genus or family. This could indicate competitive exclusion in the biofilm, assuming that closely related species occupy similar environmental niches (Stegen et al., 2013). Within *Hyphomonas*, two ASVs showed significant changes with time. ASV18 decreased with time and had higher relative abundance on concrete without steel fibers while ASV105 tended to increase with time and had higher relative abundance on concrete with steel fibers (Fig. S17). Two ASVs within *Glaciecola* showed similar, but less evident, trends. Several ASVs within the phylum *Planctomycetota* increased significantly over time (Fig. S18). Particularly ASV3, a *Planctomicrobium* sp., became dominant in systems 1, 2, and 4, reaching over 30% relative abundance. The type-strain of this genus, *Planctomicrobium piriforme*, was isolated from a boreal lake and found not to grow at NaCl concentrations above 0.5% (Kulichevskaya et al., 2015). However, ASV3 had only 88% nucleotide identity to this strain. Instead, a BLASTn search of NCBI Genbank resulted in matches with 100% nucleotide identities from both wastewater treatment systems (LR637872.1) and coastal seawater (JF948432) suggesting that this ASV represented a species that can grow in many different habitats.

4.3. Effect of concrete surface type on the microbial community

Concrete surface type influenced the biofilm community composition. The biofilm communities on the rough and smooth concrete surfaces were different to each other over the entire duration of the experiment (413 days, Fig. 3B and C). This suggests that the effects of surface topography can prevail for long periods of time, not only during colonization and early-stage biofilm formation, as previously shown for both natural and artificial surfaces (Jones and Bennett 2017; Zhang et al., 2014). However, the effects of surface topography were small. Only a limited number of ASVs were significantly different between the rough and smooth surfaces (Fig. 6). Probably, topography differences between the rough and smooth concrete were minor at the scale relevant for microbial colonization, as has also been observed for various concrete mixes (Voegel et al., 2020). Steel fiber reinforcement had greater effect on the biofilm community composition than the surface topography (Fig. 3C), with a number of ASVs having significantly different abundance in the presence of steel fibers (Fig. 6). Most of the taxa that had significantly higher abundance in the biofilms on the steel fiber reinforced concrete have unknown roles in the community. The well-known marine iron-oxidizer *Mariprofundus* within *Zetaproteobacteria* (McBeth et al., 2011) was not enriched on the concrete surfaces with steel fiber. It was only detected in a few biofilm samples on concrete without steel fibers (system 1). However, one ASV within *Magnetospiraceae*, a group of magnetotactic bacteria, was significantly more abundant in biofilms on steel-containing concrete. Magnetotactic bacteria have efficient iron-uptake systems for dissolved Fe(II) and Fe(III) and are important for iron biomineralization (Amor et al., 2020). The ASV had high relative abundance in the first sample taken on day 147 and then decreased over time. This may suggest that this bacterium contributed to metabolizing iron in the early stages of biofilm formation and then decreased in relative abundance when most of the exposed iron surface had been converted into insoluble iron oxides/hydroxides (Fig. S16). Indeed, iron hydroxide and/or iron oxyhydroxide was observed by SEM (Fig. S4) and orange deposits were seen on the surfaces of concrete containing steel fibers (Fig. 1). Other ASVs within *Portibacter*, *Rubripirellula*, and *Rhodopirellula*, also favored steel-fiber containing concrete although they were also present on concrete without steel fibers. *Portibacter* sp. has previously been found to thrive on iron slag (Ogawa et al., 2020) and *Planctomycetes*, which include *Rubripirellula* and *Rhodopirellula*, have been found in iron-hydroxide deposits in marine environments, suggesting that these microorganisms may be involved in iron metabolism (Storesund and Øvreås, 2013). Presence of iron can have systematic effects on microbial communities, that besides involving species converting iron and sulfur commonly associated with corrosion processes (Ramirez et al., 2016), also involves microorganisms capable of nitrogen cycling, as well as bacteria with less evident functions in the iron-associated microbiomes (Huang et al., 2021; Ogawa et al., 2020).

4.4. Effect of biofilms on the concrete surface

Both the SEM-analysis and the chemical composition of the water gave indications of concrete degradation in the outermost layers. There were signs of concrete transformation and little/no Ca in the outermost concrete layers, suggesting Ca dissolution (Figs. S4–S6). This was supported by consistently higher concentrations of Ca and other concrete constituents in the water after recirculation in the system for a few weeks (Fig. S8). Formation of biogenic acids near the concrete surface by the biofilm community may have assisted in the cement paste dissolution. Biogenic acids can be produced by microorganisms via a number of metabolic pathways, including conversions of sulfur, nitrogen, and organic carbon (Bertron 2014). No typical acid-producing clades of bacteria, like sulfur- and ammonia-oxidizing bacteria, were detected among the main ASVs in the biofilm communities (Fig. 5, Table S3). But even common traits, like fermentation to produce low molecular weight fatty acids from complex organic molecules, or release of CO_2, can cause concrete degradation, especially considering the elevated local concentrations in the concrete-biofilm interface (Magniont et al., 2011).

Metagenomic predictions indicated that the pathway for mixed acid fermentation was common in the biofilm (16–30% of the identified microbial taxa possessed the pathway, Supplementary data file 1), indicating that this may have been an important process contributing to the observed concrete dissolution. Interestingly, the fraction of the community having the mixed fermentation pathway decreased with time in the biofilm but not in the water phase (Fig. S19), suggesting that the biofilm growth mode selected for taxa with other pathways for organic matter turnover. And as expected, the prokaryotic TCA cycle I (and other variants of the TCA cycle, e.g. IV and V) resulting in production of CO_2, were omnipresent in the predicted metagenomes (Supplementary data file 1). It should also be noted that the metabolic potential of the large share of unidentified microbial community members cannot be predicted based on 16S rRNA genes. Hence, to fully understand the biotic mechanisms resulting in the concrete degradation, which was outside the scope of this study, other approaches like true meta-omics would be needed.

5. Conclusions

The biofilm communities on the concrete were distinctly different from the pelagic communities in the surrounding water, with limited influence of stochastic immigration. Time was the main factor shaping the biofilm communities, with increases in alpha diversity and turnover of taxa mostly driven by deterministic processes. However, specific taxa were associated with the presence/absence of iron fiber and to a lesser extent with the rough/smooth surfaces throughout the study period of 413 days, resulting in a long-lasting effect of substratum properties on biofilm communities.

Funding

This work was supported by Future Infrastructures, a research agreement between Chalmers University of Technology, Sweden, and the Norwegian Public Road Administration, Norway.

Declaration of competing interest

The authors declare that they have no known competing financial interests or personal relationships that could have appeared to influence the work reported in this paper.

Acknowledgements

The authors would like to tank Amir Saeid Mohammadi for assistance in the laboratory and the staff at the Kristineberg Marine Research Station for assistance in the collection of deep seawater. The authors acknowledge the Natural History Museum, University of Oslo for use of their SEM.

Appendix A. Supplementary data

Supplementary data to this article can be found online at https://doi.org/10.1016/j.ibiod.2022.105458.

References

Ali, M., Wang, Z.W., Salam, K.W., Hari, A.R., Pronk, M., van Loosdrecht, M.C.M., Saikaly, P.E., 2019. Importance of species sorting and immigration on the bacterial assembly of different-sized aggregates in a full-scale aerobic granular sludge plant. Environ. Sci. Technol. 53, 8291–8301. https://doi.org/10.1021/acs.est.8b07303.

Amor, M., Mathon, F.P., Monteil, C.L., Busigny, V., Lefevre, C.T., 2020. Iron-biomineralizing organelle in magnetotactic bacteria: function, synthesis and preservation in ancient rock samples. Environ. Microbiol. 22, 3611–3632. https://doi.org/10.1111/1462-2920.15098.

Anderson, M.J., 2001. A new method for non-parametric multivariate analysis of variance. Austral Ecol. 26, 32–46. https://doi.org/10.1111/j.1442-9993.2001.01070 x.

APHA, 1998. Standard Methods for the Examination of Water and Wastewater. American Public Health Association, Washington DC.

Beech, W.B., Sunner, J., 2004. Biocorrosion: towards understanding interactions between biofilms and metals. Curr. Opin. Biotechnol. 15, 181–186. https://doi.org/10.1016/j.copbio.2004.05.001.

Berrocal, C.G., 2017. Corrosion of Steel Bars in Fiber Reinforced Concrete: Corrosion Mechanisms and Structural Performance. PhD-thesis. Chalmers University of Technology, Gothenburg, Sweden.

Bertron, A., 2014. Understanding interactions between cementitious materials and microorganisms: a key to sustainable and safe concrete structures in various contexts. Mater. Struct. 47, 1787–1806. https://doi.org/10.1617/s11527-014-0433-1.

Besemer, K., Peter, H., Logue, J.B., Langenheder, S., Lindstrom, E.S., Tranvik, L.J., Battin, T.J., 2012. Unraveling assembly of stream biofilm communities. ISME J. 6, 1459–1468. https://doi.org/10.1038/ismej.2011.205.

Brislawn, C.J., Graham, E.B., Dana, K., Ihardt, P., Fansler, S.J., Chrisler, W.B., Cliff, J.B., Stegen, J.C., Moran, J.J., Bernstein, H.C., 2019. Forfeiting the priority effect: turnover defines biofilm community succession. ISME J. 13, 1865–1877. https://doi.org/10.1038/s41396-019-0396-x.

Callahan, B.J., McMurdie, P.J., Rosen, M.J., Han, A.W., Johnson, A.J.A., Holmes, S.P., 2016. DADA2: high-resolution sample inference from Illumina amplicon data. Nat. Methods 13, 581. https://doi.org/10.1038/Nmeth.3869.

Caporaso, J.G., Lauber, C.L., Walters, W.A., Berg-Lyons, D., Lozupone, C.A., Turnbaugh, P.J., Fierer, N., Knight, R., 2011. Global patterns of 16S rRNA diversity at a depth of millions of sequences per sample. Proc. Natl. Acad. Sci. U. S. A. 108 (Suppl. 1), 4516–4522. https://doi.org/10.1073/pnas.1000080107.

Caruso, G., 2020. Microbial colonization in marine environments: overview of current knowledge and emerging research topics. J. Mar. Sci. Eng. 8, 78. https://doi.org/10.3390/jmse8020078.

Caspi, R., Billington, R., Keseler, I.M., Kothari, A., Krummenacker, M., Midford, P.E., Ong, W.K., Paley, S., Subhraveti, P., Karp, P.D., 2020. The MetaCyc database of metabolic pathways and enzymes - a 2019 update. Nucleic Acids Res. 48, D445–D453. https://doi.org/10.1093/nar/gkz862.

Chao, A.N., Chiu, C.H., Jost, L., 2014. Unifying species diversity, phylogenetic diversity, functional diversity, and related similarity and differentiation measures through Hill numbers. Annu. Rev. Ecol. Evol. Syst. 45, 297–324. https://doi.org/10.3390/jmse8020078.

Chase, J.M., Myers, J.A., 2011. Disentangling the importance of ecological niches from stochastic processes across scales. Phil. Trans. Biol. Sci. 366, 2351–2363. https://doi.org/10.1098/rstb.2011.0063.

Chase, J.M., Kraft, N.J.B., Smith, K.G., Vellend, M., Inouye, B.D., 2011. Using null models to disentangle variation in community dissimilarity from variation in alpha-diversity. Ecosphere 2 (24). https://doi.org/10.1890/ES10-00117.1.

Core Team, R., 2020. R: A Language and Environment for Statistical Computing. R Foundation for Statistical Computing, Vienna, Austria.

Crawford, R.J., Webb, H.K., Truong, V.K., Hasan, J., Ivanova, E.P., 2012. Surface topographical factors influencing bacterial attachment. Adv. Colloid Interface Sci. 179, 142–149. https://doi.org/10.1016/j.cis.2012.06.015.

Dang, H.Y., Lovell, C.R., 2016. Microbial surface colonization and biofilm development in marine environments. Microbiol. Mol. Biol. Rev. 80, 91–138. https://doi.org/10.1128/Mmbr.00037-15.

Dang, H.Y., Chen, R.P., Wang, L., Shao, S.D., Dai, L.Q., Ye, Y., Guo, L.Z., Huang, G.Q., Klotz, M.G., 2011. Molecular characterization of putative biocorroding microbiota with a novel niche detection of Epsilon- and Zetaproteobacteria in Pacific Ocean coastal seawaters. Environ. Microbiol. 13, 3059–3074. https://doi.org/10.1111/j.1462-2920.2011.02583.x.

Datta, M.S., Sliwerska, E., Gore, J., Polz, M.F., Cordero, O.X., 2016. Microbial interactions lead to rapid micro-scale successions on model marine particles. Nat. Commun. 7, 11965 https://doi.org/10.1038/ncomms11965.

Dini-Andreote, F., Stegen, J.C., van Elsas, J.D., Salles, J.F., 2015. Disentangling mechanisms that mediate the balance between stochastic and deterministic processes in microbial succession. Proc. Natl. Acad. Sci. U. S. A 112, E1326–E1332. https://doi.org/10.1073/pnas.1414261112.

Douglas, G.M., Maffei, V.J., Zaneveld, J.R., Yurgel, S.N., Brown, J.R., Taylor, C.M., Huttenhower, C., Langille, M.G.I., 2020. PICRUSt2 for prediction of metagenome functions. Nat. Biotechnol. 38, 685–688. https://doi.org/10.1038/s41587-020-0548-6.

Edgar, R.C., 2016. SINTAX: a simple non-Bayesian taxonomy classifier for 16S and ITS sequences. bioRxiv, 074161. https://doi.org/10.1101/074161.

Flemming, H.C., Wuertz, S., 2019. Bacteria and archaea on Earth and their abundance in biofilms. Nat. Rev. Microbiol. 17, 247–260. https://doi.org/10.1038/s41579-019-0158-9.

Flemming, H.C., Wingender, J., Szewzyk, U., Steinberg, P., Rice, S.A., Kjelleberg, S., 2016. Biofilms: an emergent form of bacterial life. Nat. Rev. Microbiol. 14 (9), 563–575. https://doi.org/10.1038/nrmicro.2016.94.

Hagelia, P., 2011. Deterioration Mechanisms and Durability of Sprayed Concrete for Rock Support in Tunnels. PhD Thesis. TU Delft, The Netherlands.

Hayek, M., Salgues, M., Souche, J.C., Cunge, E., Giraudel, C., Paireau, O., 2021. Influence of the intrinsic characteristics of cementitious materials on biofouling in the marine environment. Sustainability 13 (5), 2625. https://doi.org/10.3390/su13052625.

Huang, Y., Xu, D., Huang, L.Y., Lou, Y.T., Muhadesi, J.B., Qian, H.C., Zhou, E.Z., Wang, B.J., Li, X.T., Jiang, Z., Liu, S.J., Zhang, D.W., Jiang, C.Y., 2021. Responses of soil microbiome to steel corrosion. NPJ Biofilms Microbiomes 7, 6. https://doi.org/10.1038/s41522-020-00175-3.

Hugerth, L.W., Wefer, H.A., Lundin, S., Jakobsson, H.E., Lindberg, M., Rodin, S., Engstrand, L., Andersson, A.F., 2014. DegePrime, a program for degenerate primer

design for broad-taxonomic-range PCR in microbial ecology studies. Appl. Environ. Microbiol. 80, 5116–5123. https://doi.org/10.1128/Aem.01403-14.
Jackson, C.R., Churchill, P.F., Roden, E.E., 2001. Successional changes in bacterial assemblage structure during epilithic biofilm development. Ecology 82, 555–566. https://doi.org/10.1890/0012-9658 (2001)082[0555:Scibas]2.0.Co;2.
Jones, A.A., Bennett, P.C., 2017. Mineral ecology: surface specific colonization and geochemical drivers of biofilm accumulation, composition, and phylogeny. Front. Microbiol. 8, 491. https://doi.org/10.3389/fmicb.2017.00491.
Jones, P.R., Cottrell, M.T., Kirchman, D., Dexter, S.C., 2007. Bacterial community structure of biofilms on artificial surfaces in an estuary. Microb. Ecol. 53, 153–162. https://doi.org/10.1007/s00248-006-9154-5.
Jost, L., 2006. Entropy and diversity. Oikos 113, 363–375. https://doi.org/10.1111/j.2006.0030-1299.14714.x.
Jost, L., 2007. Partitioning diversity into independent alpha and beta components. Ecology 88 (10), 2427–2439. https://doi.org/10.1890/06-1736.1.
Karačić, S., Wilen, B.M., Suarez, C., Hagelia, P., Persson, F., 2018. Subsea tunnel reinforced sprayed concrete subjected to deterioration harbours distinct microbial communities. Biofouling 34, 1161–1174. https://doi.org/10.1080/08927014.2018.1556259.
Konopka, A., 2009. What is microbial community ecology? ISME J. 3, 1223–1230. https://doi.org/10.1038/ismej.2009.88.
Kozich, J.J., Westcott, S.L., Baxter, N.T., Highlander, S.K., Schloss, P.D., 2013. Development of a dual-index sequencing strategy and curation pipeline for analyzing amplicon sequence data on the MiSeq Illumina sequencing platform. Appl. Environ. Microbiol. 79, 5112–5120. https://doi.org/10.1128/AEM.01043-13.
Kulichevskaya, I.S., Ivanova, A.A., Detkova, E.N., Rijpstra, W.I.C., Sinninghe Damsté, J. S., Dedysh, S.N., 2015. Planctomicrobium piriforme gen. nov., sp. nov., a stalked planctomycete from a littoral wetland of a boreal lake. Int. J. Syst. Evol. Microbiol. 65, 1659–1665. https://doi.org/10.1099/ijs.0.000154.
Liébana, R., Modin, O., Persson, F., Szabo, E., Hermansson, M., Wilén, B.M., 2019. Combined deterministic and stochastic processes control microbial succession in replicate granular biofilm reactors. Environ. Sci. Technol. 53, 4912–4921. https://doi.org/10.1021/acs.est.8b06669.
Love, M.I., Huber, W., Anders, S., 2014. Moderated estimation of fold change and dispersion for RNA-seq data with DESeq2. Genome Biol. 15, 550. https://doi.org/10.1186/s13059-014-0550-8.
Lyytimäki, J., Petersen, L.K., Normander, B., Bezák, P., 2008. Nature as a nuisance? Ecosystem services and disservices to urban lifestyle. Environ. Sci. J. Integr. Environ. Res. 5, 161–172. https://doi.org/10.1080/15693430802055524.
Magniont, C., Coutand, M., Bertron, A., Cameleyre, X., Lafforgue, C., Beaufort, S., Escadeillas, G., 2011. A new test method to assess the bacterial deterioration of cementitious materials. Cement Concr. Res. 41, 429–438. https://doi.org/10.1016/j.cemconres.2011.01.014.
McBeth, J.M., Little, B.J., Ray, R.I., Farrar, K.M., Emerson, D., 2011. Neutrophilic iron-oxidizing "Zetaproteobacteria" and mild steel corrosion in nearshore marine environments. Appl. Environ. Microbiol. 77, 1405–1412. https://doi.org/10.1128/AEM.02095-10.
Mitik-Dineva, N., Wang, J., Mocanasu, R.C., Stoddart, P.R., Crawford, R.J., Ivanova, E.P., 2008. Impact of nano-topography on bacterial attachment. Biotechnol. J. 3, 536–544. https://doi.org/10.1002/biot.200700244.
Modin, O., Liebana, R., Saheb-Alam, S., Wilén, B.M., Suarez, C., Hermansson, M., Persson, F., 2020. Hill-based dissimilarity indices and null models for analysis of microbial community assembly. Microbiome 8, 132. https://doi.org/10.1186/s40168-020-00909-7.
Natanzi, A.S., Thompson, B.J., Brooks, P.R., Crowe, T.P., McNally, C., 2021. Influence of concrete properties on the initial biological colonisation of marine artificial structures. Ecol. Eng. 159, 106104 https://doi.org/10.1016/j.ecoleng.2020.106104.
Nathaniel, O., Sam, A.R.M., Lim, N.H.A.S., Adebisi, O., Abdulkareem, M., 2020. Biogenic approach for concrete durability and sustainability using effective microorganisms: a review. Construct. Build. Mater. 261, 119664 https://doi.org/10.1016/j.conbuildmat.2020.119664.
Noeiaghaei, T., Mukherjee, A., Dhami, N., Chae, S.R., 2017. Biogenic deterioration of concrete and its mitigation technologies. Construct. Build. Mater. 149, 575–586. https://doi.org/10.1016/j.conbuildmat.2017.05.144.
Ogawa, A., Tanaka, R., Hirai, N., Ochiai, T., Ohashi, R., Fujimoto, K., Akatsuka, Y., Suzuki, M., 2020. Investigation of biofilms formed on steelmaking slags in marine environments for water depuration. Int. J. Mol. Sci. 21, 6945. https://doi.org/10.3390/ijms21186945.
Procópio, L., 2020. Microbial community profiles grown on 1020 carbon steel surfaces in seawater-isolated microcosm. Ann. Microbiol. 70, 13. https://doi.org/10.1186/s13213-020-01547-y.
Quast, C., Pruesse, E., Yilmaz, P., Gerken, J., Schweer, T., Yarza, P., Peplies, J., Glockner, F.O., 2013. The SILVA ribosomal RNA gene database project: improved data processing and web-based tools. Nucleic Acids Res. 41, D590–D596. https://doi.org/10.1093/nar/gks1219.
Ramirez, G.A., Hoffman, C.L., Lee, M.D., Lesniewski, R.A., Barco, R.A., Garber, A., Toner, B.M., Wheat, C.G., Edwards, K.J., Orcutt, B.N., 2016. Assessing marine microbial induced corrosion at Santa Catalina Island, California. Front. Microbiol. 7, 1679. https://doi.org/10.3389/fmicb.2016.01679.
Raup, D.M., Crick, R.E., 1979. Measurement of faunal similarity in paleontology. J. Paleontol. 53, 1213–1227. DOI WOS:A1979HJ45600015.
Redford, A.J., Fierer, N., 2009. Bacterial succession on the leaf surface: a novel system for studying successional dynamics. Microb. Ecol. 58, 189–198. https://doi.org/10.1007/s00248-009-9495-y.
Rognes, T., Flouri, T., Nichols, B., Quince, C., Mahe, F., 2016. VSEARCH: a versatile open source tool for metagenomics. PeerJ 18 (4), e2584. https://doi.org/10.7717/peerj.2584.
Ryley, M., Carve, M., Piola, R., Scardino, A.J., Shimeta, J., 2021. Comparison of biofouling on 3D-printing materials in the marine environment. Int. Biodeterior. Biodegrad. 164, 105293 https://doi.org/10.1016/j.ibiod.2021.105293.
Sanli, K., Bengtsson-Palme, J., Nilsson, R.H., Kristiansson, E., Alm Rosenblad, M., Blanck, H., Eriksson, K.M., 2015. Metagenomic sequencing of marine periphyton: taxonomic and functional insights into biofilm communities. Front. Microbiol. 6, 1192. https://doi.org/10.3389/fmicb.2015.01192.
Shade, A., Caporaso, J.G., Handelsman, J., Knight, R., Fierer, N., 2013. A meta-analysis of changes in bacterial and archaeal communities with time. ISME J. 7, 1493–1506. https://doi.org/10.1038/ismej.2013.54.
Song, Y., Tian, Y., Li, X., Wei, J., Zhang, H., Bond, P.L., Yuan, Z., Jiang, G., 2019. Distinct microbially induced concrete corrosion at the tidal region of reinforced concrete sewers. Water Res. 150, 392–402. https://doi.org/10.1016/j.watres.2018.11.083.
Stegen, J.C., Lin, X.J., Fredrickson, J.K., Chen, X.Y., Kennedy, D.W., Murray, C.J., Rockhold, M.L., Konopka, A., 2013. Quantifying community assembly processes and identifying features that impose them. ISME J. 7, 2069–2079. https://doi.org/10.1038/ismej.2013.93.
Stewart, P.S., 2003. Diffusion in biofilms. J. Bacteriol. 185, 1485–1491. https://doi.org/10.1128/JB.185.5.1485-1491.2003.
Storesund, J.E., Øvreås, L., 2013. Diversity of Planctomycetes in iron-hydroxide deposits from the Arctic Mid Ocean Ridge (AMOR) and description of Bythopirellula goksoyri gen. nov., sp. nov., a novel Planctomycete from deep sea iron-hydroxide deposits. Antonie Leeuwenhoek 104, 569–584. https://doi.org/10.1007/s10482-013-0019-x.
Torres-Luque, M., Bastidas-Arteaga, E., Schoefs, F., Sanchez-Silva, M., Osma, J.F., 2014. Non-destructive methods for measuring chloride ingress into concrete: state-of-the-art and future challenges. Construct. Build. Mater. 68, 68–81. https://doi.org/10.1016/j.conbuildmat.2014.06.009.
Veach, A.M., Stegen, J.C., Brown, S.P., Dodds, W.K., Jumpponen, A., 2016. Spatial and successional dynamics of microbial biofilm communities in a grassland stream ecosystem. Mol. Ecol. 25, 4674–4688. https://doi.org/10.1111/mec.13784.
Vishwakarma, V., 2020. Impact of environmental biofilms: industrial components and its remediation. J. Basic Microbiol. 60 (3), 198–206. https://doi.org/10.1002/jobm.201900569.
Vivier, B., Claquin, P., Lelong, C., Lesage, Q., Peccate, M., Hamel, B., Georges, M., Bourguiba, A., Sebaibi, N., Boutouil, M., Goux, D., Dauvin, J.-C., Orvain, F., 2021. Influence of infrastructure material composition and microtopography on marine biofilm growth and photobiology. Biofouling 37 (7), 740–756. https://doi.org/10.1080/08927014.2021.1959918.
Voegel, C., Durban, N., Bertron, A., Landon, Y., Erable, B., 2020. Evaluation of microbial proliferation on cementitious materials exposed to biogas systems. Environ. Technol. 41, 2439–2449. https://doi.org/10.1080/09593330.2019.1567610.
Wang, J., Lu, J., Zhang, Y., Wu, J., Luo, Y., 2020. Unique bacterial community of the biofilm on microplastics in coastal water. Bull. Environ. Contam. Toxicol. https://doi.org/10.1007/s00128-020-02875-0.
Wei, S.P., Jiang, Z.L., Liu, H., Zhou, D.S., Sanchez-Silva, M., 2013. Microbiologically induced deterioration of concrete - a review. Braz. J. Microbiol. 44, 1001–1007. https://doi.org/10.1590/S1517-83822014005000006.
Zhang, P., Wang, Y., Tian, R.M., Bougouffa, S., Yang, B., Cao, H.L., Zhang, G., Wong, Y. H., Xu, W., Batang, Z., Al-Suwailem, A., Zhang, X.X., Qian, P.Y., 2014. Species sorting during biofilm assembly by artificial substrates deployed in a cold seep system. Sci. Rep. 4, 6647. https://doi.org/10.1038/srep06647.
Zhou, J.Z., Ning, D.L., 2017. Stochastic community assembly: does it matter in microbial ecology? Microbiol. Mol. Biol. Rev. 81, e00002–17. https://doi.org/10.1128/MMBR.00002-17.
Zhou, J., Yin, S., Fu, Q., Wang, Q., Huang, Q., Wang, J., 2021. Microbial-induced concrete corrosion under high-salt conditions: microbial community composition and environmental multivariate association analysis. Int. Biodeterior. Biodegrad. 164, 105287 https://doi.org/10.1016/j.ibiod.2021.105287.